Proposed Extension of FETI Methods to the Boundary Elememt Technique

Richard Griffith and Kenneth Murata

Sandia National Laboratories

Proposed Extension of FETI Methods to the Boundary Element Technique

Richard Griffith
Plasma/Aerosol/Noncontinuum Process

Kenneth Murata
Modeling and Analysis

Sandia National Laboratories
P.O. B ox 5800
Albuquerque, NM 87185-0739

Abstract

One emerging threat to the national critical infrastructure is the release of chemical or biological agents in or near large complex facilities. Predictive computational models for the time-dependent transport of gas and aerosol in and around target facilities is required to effectively assess and mitigate this threat. Despite this growing need for computational flow models that can be used in extremely large, complex geometries, current computational approaches are limited to $10^7 - 10^8$ nodes. This is sufficient to model a single large interior space with a typical level of turbulence, but far less than the number of computational cells required to model all or even part of a large, modern building. The use of non-overlapping finite-element domain decomposition methods to achieve scalability with respect to problem size on massively parallel computers has been extensively developed over the past decade. In some cases, a high degree of scalability is achieved with only a single level of domain decomposition. Since a single level of domain decomposition is desirable for load balancing on massively parallel computers, a single-level method has the advantage of not introducing additional complex substructures on the problem, although special requirements may be imposed by the domain decomposition method on the nature of the subdomains to preserve scalability.

Of the many different domain decomposition methods that have been developed, the single-level finite element tearing and interconnecting (FETI) method has become recognized as an effective way to achieve good scalability in large problems. This iterative method with a built-in "coarse" problem has been developed primarily for static and time-dependent elasticity problems, with both homogeneous and highly heterogeneous material properties. However, it has also been applied to potential problems. This report discusses the extension of FETI methods to boundary element methods (BEM). The immediate motivation for this extension is the development of scalable methods for solving for the potential in BEM-based velocity-vorticity formulations of incompressible flow.

Table of Contents

1 Introduction

One emerging threat to the national critical infrastructure is the release of chemical or biological agents in or near large complex facilities. Predictive computational models for the time-dependent transport of gas and aerosol in and around target facilities is required to effectively assess and mitigate this threat. Despite this growing need for computational flow models that can be used in extremely large, complex geometries, current computational approaches are limited to $10^7 - 10^8$ nodes. This is sufficient to model a single large interior space with a typical level of turbulence, but far less than the number of computational cells required to model all or even part of a large, modern building. After significant investigation, a computational approach to provide this modeling capability was explored under a 3 year LDRD. Unfortunately, when Sandia's FY00 LDRD budget was reduced from 6% to 4% the present work was abruptly cancelled just after the first year had been completed. The present report discusses the work that was completed before the end of the project, and represents a useful foundation if the project is refunded under a future LDRD. However, it does not describe a completed research effort.

The use of non-overlapping finite-element domain decomposition methods to achieve scalability with respect to problem size on massively parallel computers has been extensively developed over the past decade. In some cases, a high degree of scalability is achieved with only a single level of domain decomposition. Since a single level of domain decomposition is desirable for load balancing on massively parallel computers, a single-level method has the advantage of not introducing additional complex substructures on the problem, although special requirements may be imposed by the domain decomposition method on the nature of the subdomains to preserve scalability.[*]

Of the many different domain decomposition methods that have been developed,[1] the single-level finite element tearing and interconnecting (FETI) method[2] has become recognized as an effective way to achieve good scalability in large problems. This iterative method with a built-in "coarse" problem has been developed primarily for static and time-dependent elasticity problems, with both homogeneous and highly heterogeneous material properties. However, it has also been applied to potential problems. For the finite element applications the condition number for the FETI method with optimal preconditioning is typically stated as:

$$\kappa = \vartheta\left(1 + \log^m\left(H/h\right)\right)$$
(1)

where H is the length scale of the subdomains, h is the length scale of the mesh, and m = 3 or 2, depending on the presence or absence, respectively of edge or corner cross-ties in the problem.

---

[*] Such requirements for finite element methods have been studied extensively. However, the requirements with respect to the boundary element technique will not be discussed here but will be the subject of future investigations.

Note that the condition number κ is independent of the number of subdomains. This is important for the type of scalability of interest here, which is embodied in the so-called speed-up factor. A condition number independent of the number of subdomains means a problem can be set up with a given number of subdomains per processor, each with a given number of degrees of freedom (DOF). According to Equation (1), the number of processors and thus the problem size can be increased without changing the condition number. This translates into linear scaling of the speed-up factor with problem size, provided, of course, that one can neglect the effort required to solve the "coarse" or global aspects of the problem which are essential to a condition number that is independent of subdomain number.

In a FETI method, a relatively small global "coarse" problem arises naturally and is related to the collective null-spaces that are often present in stiffness matrix ($\mathbf{K}^{(s)}$) for each subdomain. This coarse problem is solved twice per iteration cycle (in the finite-element version of FETI) and the information from this solution is propagated throughout the subdomains. The DOF in this coarse problem correspond to the rigid-body translational and rotational modes of a subdomain for an elasticity problem and to the overall constant term in the potential within a subdomain for a potential problem, whenever such "modes" are not fixed by external Dirichlet boundary conditions. Thus, the coarse problem can contain up to 6 DOF per subdomain in an elasticity problem and up to one DOF per subdomain in a potential problem.

The present memo discusses the extension of FETI methods to boundary element methods (BEM). The immediate motivation for this extension is the development of scalable methods for solving for the potential in BEM-based velocity-vorticity formulations of incompressible flow. The FETI method has been selected for generalization to BEM because of the fact that the former utilizes Lagrange multipliers to enforce continuity constraints on the boundary between subdomains. It is well known that these Lagrange multipliers play the role of boundary tractions in an elasticity problem and velocities in a potential problem. This formulation has a logical extension to BEM, which generates an inherently mixed formulation with explicit displacement and traction, or potential and normal potential velocity, terms. (Hereafter, all velocities in the following discussion will be assumed to refer to the normal component at the boundary, unless otherwise specified.)

This mixed nature is apparent at the internal interfaces between subdomains because both the displacements and tractions (potentials and potential velocities) appear as unknowns along such boundaries. The logical extension of FETI to BEM is to treat the potential velocities in a manner analogous to the Lagrange multipliers in the FETI method. It may be possible to extend other finite element domain decomposition methods to BEM, but the extension is less obvious since one must first deal with (i.e., eliminate) one of the unknowns (e.g., the potential velocities) obtained in BEM at the internal interfaces. One likely candidate besides FETI is the finite element Balancing Domain Decomposition (BDD) method,[3] which can be considered the "dual space" formulation to FETI. In contrast to FETI, BDD deals strictly with the displacement (potential) degrees of freedom. Successful extensions to BEM of such related methods cannot be ruled out and may be considered in more detail at a later date.

2 The Proposed BEM Formulation

A key step in the development of a velocity-vorticity-based formulation of incompressible flow is the solution of a potential problem, in which the potential is chosen to satisfy external boundary conditions on the potential and velocity. To do this within a FETI-like formulation, we assume that a non-overlapping domain decomposition of the entire domain Ω has created N_s subdomains, which we denote by Ω_s. In what follows we distinguish segments of the external domain boundary from internal interfaces between subdomains. Figure 1 shows segments of the internal interfaces between subdomains and the pairing of the internal interface nodes between adjacent subdomains. Note that a discontinuous BEM representation is assumed to be used at edges and corners between subdomains (as opposed to planar faces) so that node multiplicities on the internal interfaces (i.e. the number of subdomains that share an interface node) are always equal to 2.

In the derivation of the subdomain governing equation (Equation (4) below), velocity continuity conditions are imposed between subdomains to eliminate one velocity unknown between the node pairs in Figure 1. In contrast, the enforcement of continuity of the potential between node pairs generates the system equation (essentially, Equation (7)), and since this equation is solved interatively, continuity of the potential is achieved only at convergence.

In the following, we will for simplicity neglect compressibility effects and consider the interface velocity v to be composed of a potential part and vorticity-induced part, $v = v_\varphi + v_\omega$, where as usual

$$v_\omega^{(s)} = -\frac{1}{4\pi} \mathbf{n} \cdot \int_{\Omega_s} \frac{(\mathbf{x} - \mathbf{x'}) \times \boldsymbol{\omega}}{r^3} dR'_s$$

(2)

where $\mathbf{n}$ is the outward normal of Ω_s and $\boldsymbol{\omega}$ is the vorticity. Note that the vorticity contributions to the velocity are treated in a local manner; only the vorticity internal to a subdomain is considered to contribute to the velocity $v_\omega^{(s)}$ defined for that subdomain. The effects of the vorticity external to a given subdomain are assumed to be included in the potential velocity v_φ. Consequently, the continuity conditions on the normal velocity apply to the total normal velocity at the internal interface between two subdomains i and j and not just the potential part:

$$v_\omega^{(i)} + v_\varphi^{(i)} = -v_\omega^{(j)} - v_\varphi^{(j)}$$

(3)

In the following, we will use notation that parallels that in Reference 2 to the extent possible. In contrast to FEM, the BEM formulation is inherently mixed and for subdomain s generates a governing equation of the form

$$\mathbf{K}^{(s)}\mathbf{u}^{(s)} = -\mathbf{J}^{(s)}\mathbf{B}^{(s)^T}\mathbf{q} + \mathbf{f}^{(s)}$$

(4)

where $\mathbf{u}^{(s)}$ is a generalized vector of unknowns, consisting of unknown external boundary potential velocities, if any exist for subdomain s; unknown external boundary potentials, if any; and unknown internal interface potentials for s; $\mathbf{q}$ is a global vector of length n_I consisting of one unknown potential velocity per node pair along all internal interfaces between subdomains; and $\mathbf{K}^{(s)}$ and $\mathbf{J}^{(s)}$ are the coefficient matrices associated with $\mathbf{u}^{(s)}$ and $\mathbf{B}^{(s)T}\mathbf{q}$, respectively. (The structure of these vectors and matrices will be discussed more fully in the next section.) The matrix $\mathbf{B}^{(s)}$ is the signed Boolean matrix of dimension $n_s \times n_I$, that when multiplied into $\mathbf{u}^{(s)}$ extracts the latter's restriction to the internal interfaces of the domain decomposition. The dimension n_s is the total number of unknowns associated with subdomain s, including the unknown potentials and potential velocities on the external boundary segments and unknown potentials on the internal interfaces but excluding the potential velocities on the internal interfaces. Note that, by definition, unknowns in $\mathbf{u}^{(s)}$ corresponding to the external boundary are multiplied by zero entries in $\mathbf{B}^{(s)}$ and are ignored in this restriction. The sign applied to the restriction is determined by the +- sign pairing assigned to each node pair. (In Figure 1 this sign pairing is shown to be assigned on a subdomain by subdomain basis, although this is not necessary.) This pairing determines the arbitrary direction of positive velocity across the boundary. The vector $\mathbf{f}^{(s)}$ is determined from values of v_ω at the subdomain interfaces and from the Dirichlet and Neumann boundary conditions on any external boundary segments that are included in the subdomain.

In Equation (4), the vector $\mathbf{q}$ plays the role of the Lagrange multiplier vector λ in the FETI formulation.[2] Note that the organization of unknowns in Equation (4) reflects the fact that the roles of $\mathbf{u}$ and $\mathbf{q}$ in the FETI solver are different. In the FETI method the $\mathbf{q}$ vector is solved iteratively, and at each step of the $\mathbf{q}$ iteration, the $\mathbf{u}^{(s)}$ vector is solved (typically directly) using the $\mathbf{q}$ values for that iteration as boundary conditions. This differentiation of roles is a key distinguishing feature of a Neumann-Neumann iterative method. In contrast, in conventional BEM all unknowns are treated on the same footing and are accommodated within one large system matrix.

It should be noted that Neumann-Neumann and related methods to date have been applied only to a limited extent and with limited success to BEM.[4] One reason is that published BEM-specific methods, at least those known to the author, do not deal with the null spaces typically present in $\mathbf{K}^{(s)}$ for pure Neumann boundary conditions, and thus the published Neumann-Neumann methods cannot be used for domain decompositions with interior subdomains. A related method, the Dirichlet-Dirichlet approach, does not lead to singular matrix for internal subdomains but seems to converge very slowly even for a handful of subdomains.[4] This may be related to the fact that a suitable "coarse" problem for global information propagation has not been used in conjunction with the BEM-specific techniques.

The general solution of Equation (4) for one subdomain may be written as

$$\mathbf{u}^{(s)} = \mathbf{K}^{(s)^+}\left(\mathbf{f}^{(s)} - \mathbf{J}^{(s)}\mathbf{B}^{(s)^T}\mathbf{q}\right) + \mathbf{R}^{(s)}\boldsymbol{\alpha}^{(s)}$$

(5)

where $\mathbf{K}^{(s)+}$ is the generalized inverse of $\mathbf{K}^{(s)}$ if $\mathbf{K}^{(s)}$ is singular and the inverse of $\mathbf{K}^{(s)}$ if $\mathbf{K}^{(s)}$ is not singular. (Although methods to solve for the generalized inverse have been developed for FETI applications, they will not be discussed here.) If $\mathbf{K}^{(s)}$ is singular, then $\mathbf{R}^{(s)}$ is the matrix whose columns consist of the vectors that span the null space and $\boldsymbol{\alpha}^{(s)}$ is the amplitude of the various null space vectors in the solution. The subdomains with singular $\mathbf{K}^{(s)}$ are called "floating." In elasticity problems such subdomains arise whenever the 6 possible rigid body modes for a subdomain are not fully pinned by external Dirichlet boundary conditions. For potential problems, such subdomains are those that do not include an external boundary segment with Dirichlet boundary conditions. Thus, the total number of degrees of freedom represented by the null spaces includes up to 6 DOF per floating subdomain for elasticity problems and one DOF per floating subdomain for potential problems. For floating subdomains in potential problems, $\mathbf{R}^{(s)}$ consists of just a single column with the same nonzero value for all entries, representing the fact that the potential within a subdomain with pure Neumann boundary conditions is not defined to within an overall constant.

The condition for the solution in Equation (5) to exist is that the quantity in brackets in that equation be orthogonal to the null space of $\mathbf{K}^{(s)}$, whenever such a space exists for s:

$$\mathbf{R}^{(s)^T}\left(\mathbf{f}^{(s)} - \mathbf{J}^{(s)}\mathbf{B}^{(s)^T}\mathbf{q}\right) = 0$$

(6)

This condition is known as the equilibrium condition, or equivalently, the flux conservation condition in a potential problem. As discussed above, for a potential problem, $\mathbf{R}^{(s)}$ is just a vector with the same value for all entries. Thus, the above equation is equivalent to a column sum of the vector quantity defined by the brackets.

The system equation is formed from the continuity condition on the potential at the internal subdomain interfaces. First, recall that $\mathbf{B}^{(s)}$ restricts a vector to the internal interfaces of the domain decomposition. It should be clear from the discussion above and also in the following section that the entries of $\mathbf{u}^{(s)}$ corresponding to the internal interfaces represent only potentials, not potential velocities. Thus, the continuity condition for potentials across the internal boundaries can be written as

$$\sum_{s=1}^{N_S}\mathbf{B}^{(s)}\mathbf{u}^{(s)} = 0$$

(7)

When $\mathbf{u}^{(s)}$ from Equation (5) is substituted into the above equation and Equation (6) is taken into account, one obtains a system equation of the form

$$
\begin{bmatrix} \mathbf{F}_I & -\mathbf{G}_I \\ -\widetilde{\mathbf{G}}_I^{\ T} & \mathbf{0} \end{bmatrix} \begin{bmatrix} \mathbf{q} \\ \boldsymbol{\alpha} \end{bmatrix} = \begin{bmatrix} \mathbf{d} \\ -\mathbf{e} \end{bmatrix}
$$
(8)

where

$$
\mathbf{F}_I = \sum_{s=1}^{N_S} \mathbf{B}^{(s)} \mathbf{K}^{(s)^+} \mathbf{J}^{(s)} \mathbf{B}^{(s)T}
$$

$$
\mathbf{d} = \sum_{s=1}^{N_S} \mathbf{B}^{(s)} \mathbf{K}^{(s)^+} \mathbf{f}^{(s)}
$$

$$
\mathbf{G}_I = \begin{bmatrix} \mathbf{G}_I^{(1)} & \cdots & \mathbf{G}_I^{(N_f)} \end{bmatrix}
$$

$$
\widetilde{\mathbf{G}}_I = \begin{bmatrix} \widetilde{\mathbf{G}}_I^{(1)} & \cdots & \widetilde{\mathbf{G}}_I^{(N_f)} \end{bmatrix}
$$

$$
\boldsymbol{\alpha} = \begin{bmatrix} \boldsymbol{\alpha}^{(1)} & \cdots & \boldsymbol{\alpha}^{(N_f)} \end{bmatrix}^T
$$

$$
\mathbf{e} = \begin{bmatrix} \mathbf{f}^{(1)^T} \mathbf{R}^{(1)} & \cdots & \mathbf{f}^{(N_f)^T} \mathbf{R}^{(N_f)} \end{bmatrix}^T
$$

where N_f is the number of floating subdomains, $\mathbf{G}_I^{(s)} = \mathbf{B}^{(s)} \mathbf{R}^{(s)}$, and $\widetilde{\mathbf{G}}_I^{(s)} = \mathbf{B}^{(s)} \mathbf{J}^{(s)T} \mathbf{R}^{(s)}$.

As discussed in Reference 2, the coupling to the null space (i.e., the $\boldsymbol{\alpha}$ terms) in Equation (8) can be formally eliminated through projection operator methods. We first write $\mathbf{q}$ as

$$
\mathbf{q} = \mathbf{q}^0 + \mathbf{P}\widetilde{\mathbf{q}}
$$
(9)

where $\mathbf{q}^0$ is a particular solution of $\widetilde{\mathbf{G}}_I^{\ T}\mathbf{q} = \mathbf{e}$ of the form

$$
\mathbf{q}^0 = \mathbf{G}_I \left(\widetilde{\mathbf{G}}_I^{\ T} \mathbf{G}_I \right)^{-1} \mathbf{e}
$$
(10)

and $\mathbf{P}$ is the (non-orthogonal) projection operator

$$
\mathbf{P} = \mathbf{I} - \mathbf{G}_I (\widetilde{\mathbf{G}}_I^{\ T} \mathbf{G}_I)^{-1} \widetilde{\mathbf{G}}_I^{\ T}
$$
(11)

Note that $\mathbf{P}^T \neq \mathbf{P}$ and also $\widetilde{\mathbf{G}}_I^{\ T}\mathbf{P} = \mathbf{P}\mathbf{G}_I = 0$. The non-orthogonality of $\mathbf{P}$ is a consequence of the non-symmetric form of Equation (8) with respect to the off-diagonal subblocks (i.e., $\widetilde{\mathbf{G}}_I \neq \mathbf{G}_I$). (Note that although non-orthogonal projection operators are

also discussed in Reference 2, the non-orthogonality is explicitly introduced through the matrix $\mathbf{Q}$ defined in that reference. As discussed there, the use of certain $\mathbf{Q}$s (not equal to the identity matrix) helps to preserve scalability in heterogeneous FETI problems. The use a matrix analogous to $\mathbf{Q}$ does not appear to be possible for BEM because the non-symmetric off-diagonal subblocks in Equation (8) require that the projection operator be applied somewhat differently than in Reference 2.)

The substitution of Equations (9)-(11) into Equation (8) and left multiplication of the first row of Equation (8) by $\mathbf{P}$ (not $\mathbf{P}^{\mathrm{T}}$) lead to the equation

$$\mathbf{P}\,\mathbf{F}_{\mathrm{I}}\mathbf{P}\,\widetilde{\mathbf{q}} = \mathbf{P}\left(\mathbf{d} - \mathbf{F}_{\mathrm{I}}\,\mathbf{q}^{0}\right)$$

(12)

Also, one can show that the second row of Equation (8) (the equilibrium or flux conservation condition) is identically satisfied for any $\widetilde{\mathbf{q}}$. These are the principal new results of this document.

Before discussing the structure of the BEM matrices, the nature of the inherent "coarse" problem in FETI methods should be discussed further. This "coarse" problem is essentially embodied in the effects of the inverse in Equation (11). The square matrix $\widetilde{\mathbf{G}}_{\mathrm{I}}{}^{\mathrm{T}}\mathbf{G}_{\mathrm{I}}$ has a dimension equal to the total number of degrees of freedom represented by the null spaces in the problem. Although this matrix is sparse, its inverse is fully populated and serves to propagate information between all subdomains whenever the projection operator is applied. This global propagation is the type of behavior expected from a "coarse" problem, if it is to substantially enhance the conditioning of the problem overall.

3 Structure of the BEM Matrices

The structure of the **K** and **J** matrices is determined from application of standard BEM to a subdomain. There are in general four types of unknowns when external boundary conditions are taken into account: (1) external boundary potential velocities for nodes at which Dirichlet boundary conditions are applied, (2) external boundary potentials for nodes at which Neumann boundary conditions are applied, (3) internal interface potentials, defined separately on the two sides of the interface, and (4) internal interface potential velocities. Note that if a subdomain is strictly an interior one and does not include segments of the external domain boundary, the first two types of unknowns will be absent for that subdomain. As discussed above, the continuity condition for the interface potentials on the two sides of an internal interface is imposed as a separate condition and is equivalent to the system equation (see Equations (7) and (8)).

In the derivation of Equation (4), it was assumed that terms in the BEM governing equation containing the first three types of unknowns enumerated above were brought to the left side of Equation (4). We also assume for simplicity of notation that $\mathbf{u}^{(s)}$ consists of unknowns for the subdomain s that are grouped in the order given. The first part of $\mathbf{u}^{(s)}$ then consists of a vector of external boundary unknown DOFs

$$\mathbf{u}_i^{(s)} = \begin{bmatrix} \mathbf{q}_i^{(s)} \\ \boldsymbol{\varphi}_i^{(s)} \end{bmatrix}$$

(13)

where $\mathbf{q}_i^{(s)}$ denotes the external boundary potential velocities and $\boldsymbol{\phi}_i^{(s)}$ the external boundary potentials, and the second part consists of the internal interface potentials for that subdomain

$$\mathbf{u}_b^{(s)} = \boldsymbol{\varphi}_b^{(s)}$$

(14)

In what follows we will use a block form corresponding to the decomposition

$$\mathbf{u}^{(s)} = \begin{bmatrix} \mathbf{u}_i^{(s)} \\ \mathbf{u}_b^{(s)} \end{bmatrix}$$

(15)

The use of the subscripts "i" and "b" follows the notation used in Reference 2. The subscript "i" stands for a DOF that is "internal" to a subdomain; i.e., not defined on the interface between two subdomains. The subscript "b" on the other hand denotes a DOF at an internal interface (i.e., boundary). The rationale for this notation is that in the finite-element method, the "internal" DOFs correspond primarily to the interior nodes of a subdomain. In a BEM, there are no nodes except on the subdomain boundaries, but one must take into account the fact that the unknowns corresponding to segments of the

external boundary play the same role as an "internal" unknowns. Thus, we continue to use this notation, although it is somewhat confusing in the present application.)

In Equation (4), $\mathbf{q}$ is the internal interface potential velocity vector, consisting of one DOF for each internal interface node pair. How this vector is defined is somewhat arbitrary. For definiteness, this can be chosen as the outward normal potential velocity on the "minus" side of an interface pair. The continuity condition on the total velocity, Equation (3), can then used to define the potential velocity on the "plus" side of the interface. Thus the same unknown can be used on the two sides of the interface, provided the sum of the vorticity terms is incorporated into the "plus" side $\mathbf{f}^{(s)}$.

With respect to the subblocks shown in Equation (15), one can write

$$\mathbf{K}^{(s)} = \begin{bmatrix} \mathbf{K}_{ii}^{(s)} & \mathbf{K}_{ib}^{(s)} \\ \mathbf{K}_{bi}^{(s)} & \mathbf{K}_{bb}^{(s)} \end{bmatrix}$$

(16)

and

$$\mathbf{J}^{(s)} = \begin{bmatrix} 0 & \mathbf{J}_{ib}^{(s)} \\ 0 & \mathbf{J}_{bb}^{(s)} \end{bmatrix}$$

(17)

The first column of the $\mathbf{J}^{(s)}$ matrix has been set to zero since $\mathbf{J}^{(s)}$ multiplies $\mathbf{B}^{(s)T}$, which has non-zero entries only for internal interface DOFs. (Recall that the unknown potential velocities on external boundaries were taken to the left side of Equation (4) and are considered lumped into the $\mathbf{u}^{(s)}$ vector.)

Note that the form of flux conservation condition given in Equation (6) depends in part on the definition of $\mathbf{J}^{(s)}$. This matrix can vary, for example, depending on whether the singular or hypersingular form of the boundary integral equation is used, or whether the rows in the discretized matrix equations have been multiplied by some arbitrary factors. While it is not clear why this ambiguity should exist, $\mathbf{J}^{(s)}$ should presumably be chosen so that Equation (6) is equivalent to the conventional flux conservation equation. The natural formulation to use in this respect is the Galerkin form of the hypersingular equation, since it can be shown to produce the conventional flux conservation equation, provided column-sum relations are preserved in the numerical evaluation of the singular integral contributions to $\mathbf{J}^{(s)}$. Whether other boundary integral formulations are also appropriate is still being investigated.

13

4 Modified CGSTAB Solver

In Table I we illustrate how an iterative unsymmetric matrix solver could be modified to deal with the presence of the projection operators in Equation (12). We have chosen CGSTAB for illustration.[5] Other methods would presumably be treated in an analogous manner, but may require application of both $\mathbf{P}$ and $\mathbf{P}^T$. The results of Table I are given without derivation for illustration only (for example, to show the number and nature of the projection steps). Aside from the inherent differences between the symmetric conjugate gradient and CGSTAB methods, the steps outlined are similar to the preconditioned conjugate projected gradient (PCPG) algorithm for symmetric matrices presented in Reference 6. In either approach, the function of projection operator is to ensure that the equilibrium or flux conservation condition is satisfied after each iteration. This follows in the present case because $\mathbf{q}^0$ satisfies this equation and each term added to $\mathbf{q}$ is premultiplied by $\mathbf{P,}$ and $\widetilde{\mathbf{G}}^T\mathbf{P} = 0$. One can conclude from Table I that projection operators must be applied four times per iteration cycle for the CGSTAB method, compared to twice per cycle in the PCPG algorithm.

5 The Optimal Preconditioner Matrix

The existence of an optimal choice for the preconditioner $\overline{\overline{F}}_I^{-1}$ appearing in Table I — i.e., one that gives a poly-logarithmic condition number similar to Equation (1) — has not been demonstrated for the extension of FETI to BEM discussed here. However, the likely choice for such a preconditioner can be deduced from arguments similar to those given in Reference 6 for the FETI optimal preconditioner. This preconditioner averages over each internal interface the change in internal interface tractions (potential velocities) corresponding to given changes in the displacements (potentials), assuming that each subdomain can be treated independently and that the "internal" DOFs are free to adapt to the change.

In the present case this candidate optimal preconditioner can be shown to have the form

$$\overline{\overline{F}}_I^{-1} = \sum_{s=1}^{N_S} \mathbf{W}^{(s)} \, \mathbf{B}^{(s)} \begin{bmatrix} 0 & 0 \\ 0 & \mathbf{S}_{bb}^{(s)} \end{bmatrix} \mathbf{B}^{(s)\mathrm{T}} \mathbf{W}^{(s)}$$

(18)

where

$$\mathbf{S}_{bb}^{(s)} = \left[\mathbf{J}_{bb}^{(s)} - \mathbf{K}_{bi}^{(s)} \, \mathbf{K}_{ii}^{(s)^{-1}} \mathbf{J}_{ib}^{(s)} \right]^{-1} \left[\mathbf{K}_{bb}^{(s)} - \mathbf{K}_{bi}^{(s)} \, \mathbf{K}_{ii}^{(s)^{-1}} \mathbf{K}_{ib}^{(s)} \right]$$

is a straightforward generalization of the conventional expression for the Shur complement and $\mathbf{W}^{(s)}$ is the diagonal "topological scaling" matrix,[2,6] with diagonal entries equal to 1/n, where n is the node multiplicity, or the number of subdomains sharing the corresponding internal interface node. If, as discussed above, discontinuous boundary elements are used at all edges and corners between subdomains, then n = 2 for all internal interface nodes. In the above equation $\mathbf{W}^{(s)}$ in this case has the effect of splitting the displacement (potential) difference between subdomains and averaging the resulting tractions (potential velocities) at the interface.

6 Summary

A proposal has been given for the extension of FETI methods to BEM. The basic equations for such an extension have been derived, and the modifications needed in an unsymmetric matrix iterative solver to handle the projection operators arising in the extension have been illustrated. A likely candidate for the optimal preconditioner in the extension to BEM has also been suggested, but the scalability properties of this preconditioner remain to be demonstrated, either by theoretical or numerical means.

7 References

1. See, for example, J. Xu and J. Zou, "Some Nonoverlapping Domain Decomposition Methods," SIAM Review, <u>40</u>, No. 4, pp 857-914, December 1998.

2. M. J. Bhardwaj et al., "Application of the FETI Method to ASCI Problems: Scalability Results on a Thousand Processors and Discussion of Highly Heterogeneous Problems," SAND99-0785J, Sandia National Laboratories, March 1999.

3. J. Mandel, "Balancing Domain Decomposition," Comm. Appl. Num. Methods, <u>9</u>, pp 233-241, 1993.

4. N. Kamiya, H. Iwase, and E. Kita, "Parallel Implementation of Boundary Element Method with Domain Decomposition," Engineering Analysis with Boundary Elements, <u>18</u>, pp 217-222, 1996.

5. J. H. Ferziger and M. Peric, <u>Computational Methods for Fluid Dynamics</u>, Springer, New York, 1996.

6. D. J. Rixen and C. Farhat, "A Simple and Efficient Extension of a Class of Substructure Based Preconditioners to Heterogeneous Structural Mechanics Problems, Int. Journal for Num. Methods in Eng., <u>44</u>, pp 489-516, (1999).

Table I. Illustration of the use of the projection operator in the CGSTAB solver

_____

1. Initialize

$$\mathbf{q}^0 = \mathbf{G}_I \, (\tilde{\mathbf{G}}_I{}^T \mathbf{G}_I)^{-1} \mathbf{e}$$
$$\mathbf{r}^0 = \mathbf{P}\,(\mathbf{d} - \mathbf{F}_I \mathbf{q}^0)$$
$$\mathbf{x}^0 = 0; \ \mathbf{p}^0 = 0; \ k=0$$

2. Advance $k = k+1$ and evaluate

$$\beta^k = \mathbf{r}^0 \cdot \mathbf{r}^{k-1}$$
$$\omega^k = (\beta^k \gamma^{k-1}) / (\alpha^{k-1} \beta^{k-1})$$
$$\mathbf{p}^k = \mathbf{r}^{k-1} + \omega^k (\mathbf{p}^{k-1} - \alpha^{k-1} \mathbf{x}^{k-1})$$

3. Precondition $\mathbf{a} = \overline{\mathbf{F}}_I^{-1} \mathbf{p}^k$

   Project $\mathbf{z} = \mathbf{P}\,\mathbf{a}$

4. Calculate $\mathbf{b} = \mathbf{F}_I \mathbf{z}$

$$\text{Project } \mathbf{x}^k = \mathbf{P}\,\mathbf{b}$$
$$\gamma^k = \beta^k / (\mathbf{x}^k \cdot \mathbf{r}^0)$$
$$\mathbf{v} = \mathbf{r}^{k-1} - \gamma^k \mathbf{x}^k$$

5. Precondition $\mathbf{c} = \overline{\mathbf{F}}_I^{-1} \mathbf{v}$

   Project $\mathbf{y} = \mathbf{P}\,\mathbf{c}$

6. Calculate $\mathbf{g} = \mathbf{F}_I \mathbf{y}$

$$\text{Project } \mathbf{w} = \mathbf{P}\,\mathbf{g}$$
$$\mathbf{r}^k = \mathbf{v} - \gamma^k \mathbf{w}$$
$$\alpha^k = (\mathbf{w} \cdot \mathbf{r}^k) / (\mathbf{w} \cdot \mathbf{w})$$
$$\mathbf{q}^k = \mathbf{q}^{k-1} + \gamma^k \mathbf{z} + \alpha^k \mathbf{y}$$

7. Repeat items (2) - (6) until converged

_____
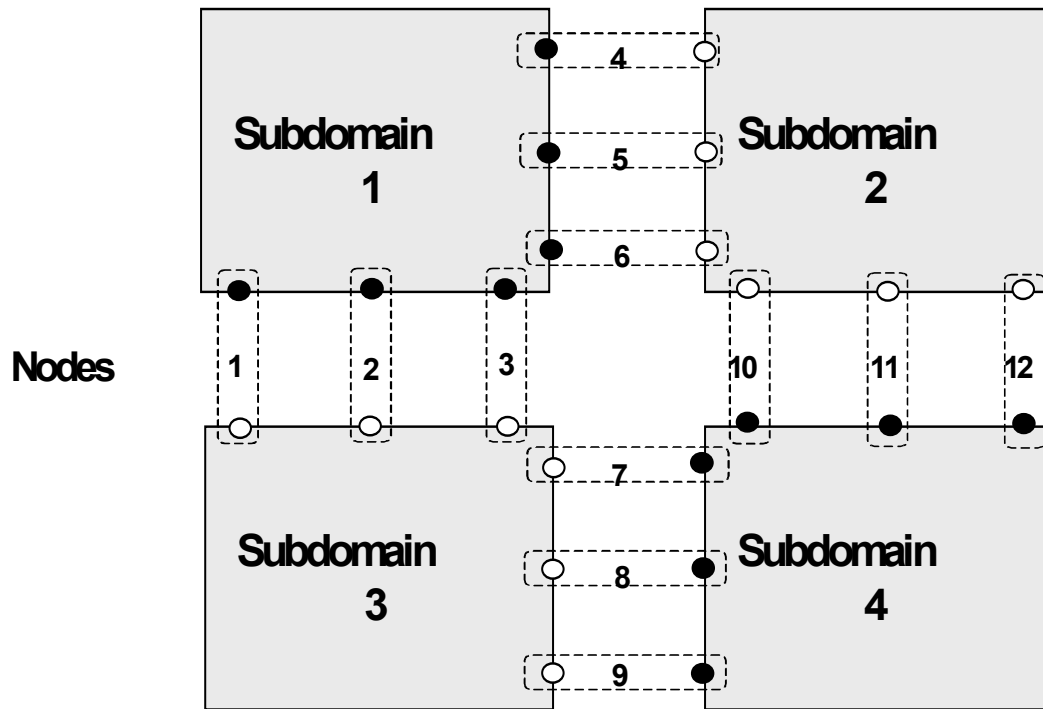
Figure 1. Illustration of node pairing at the internal interfaces between subdomains. Note the position of the solid/open dots defines the sign convention assigned to the nodes on either side of the interface (e.g., solid = +; open = -).

8 Appendix A

Powerpoint presentation attached.

Transport and Fate Simulation of Chem/Bio Agents in Critical Infrastructures

Ken Murata, Mike Glass, Sam Subia,
Fred Gelbard, Rod Schmidt, and
Richard Griffith

ESRF LDRD Review
August 18, 1999

Sandia National Laboratories

Organization of Talk

- **Introduction**

- **The multi-zone approach**

- **A highly scalable finite element (FE) domain decomposition method**

- **Development of an analogous method for boundary elements (BE)**

- **3D benchmark calculation**

Sandia National Laboratories

What is Transport and Fate?

- Transport and Fate refers to the time-dependent and spatially varying concentrations of Chem/Bio agents that develop following a release. The focus here is on interior transport in large critical infrastructures (airports, convention centers, high-rise buildings, etc.)

- The ability to model the interior transport of agents is critical to a variety of analyses involving risk assessment, evacuation planning, mitigation measures, sensor placement, building hardening, agent viability, etc.

Sandia National Laboratories

Why Focus on Interior Transport in a LDRD?

- ■ Generally, the interior flow in buildings is turbulent (a flow of 1 ft/s with a characteristic length of 20 ft gives Re ~ 10^5) and therefore difficult to model.

- ■ Current calculations seem to have a practical limit of 10^7 - 10^8 nodes.

- ■ The consensus appears to be that this is sufficient to model at most a "large" room with a typical level of turbulence; therefore only a small part of a large infrastructure can currently be resolved.

Sandia National Laboratories

LDRD Objectives

■ **The principal objective is to develop methods, within a velocity-vorticity flow formulation, that significantly extend the size of interior flow problem that can be treated. A secondary objective is to characterize the turbulence and turbulent mixing of interior flows.**

■ **Principal difficulty is that conventional boundary element methods (BEM) are not scalable. (Storage ~ N^2 ; direct solver CPU time ~ N^3)**

■ **Focus of the LDRD is to develop and implement a scalable BE method, using domain decomposition, or multi-zone, techniques**

Sandia National Laboratories

Illustration of the Multi-Zone Concept

Single-Zone →

Two-Zone →

Multi-Zone →

Sandia National Laboratories
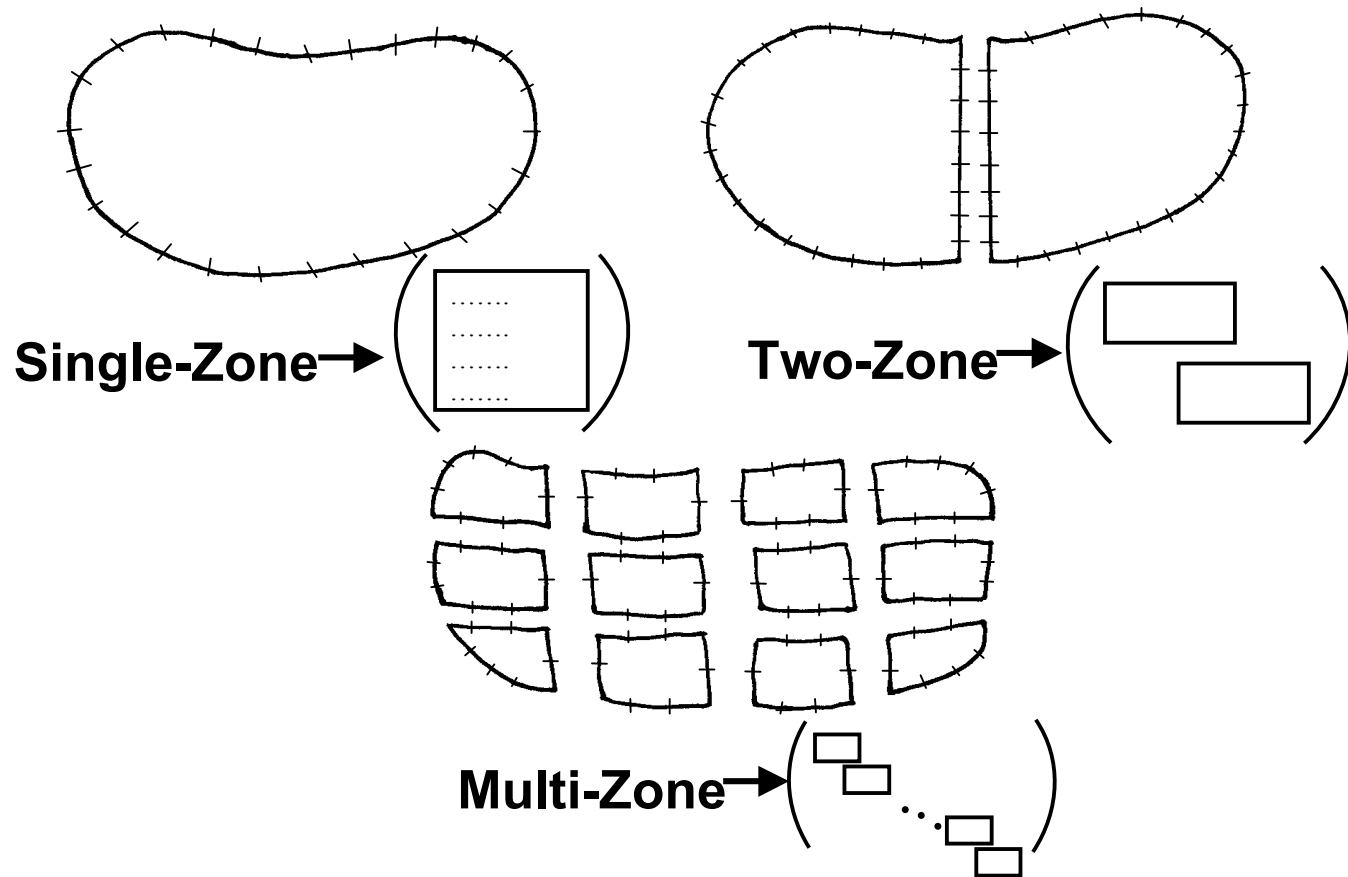
Results of Literature Survey

- **Current multi-zone solution techniques for BEM methods are extremely limited, relative to FE**

    - System-matrix assembly techniques, which typically use a direct solver. Use of iterative solvers seems to be extremely limited.

    - Iterative Schwarz techniques. These apparently do not use a coarse problem or deal with singular Neumann-only subdomains.

- **Some recent FE domain decomposition methods have achieved high scalability through proper treatment of Neumann singularities, use of a coarse problem and optimal preconditioners**

Sandia National Laboratories

The Scalable FETI* Method

- **An FE method under development since the early 90's**

- **Development has primarily been toward static and dynamic structural analysis, including plate and shell problems and highly heterogeneous applications**

- **A highly scalable solver has been developed for such applications and also for potential problems**

- **Recently, a FETI solver has been incorporated into the Sandia SALINAS elasticity code, in a joint effort with the University of Colorado**

*Finite Element Tearing and Interconnecting

Sandia National Laboratories

FETI Features

- **Lagrange multipliers, in conjunction with minimization principles, are used to enforce subdomain continuity**

- **The condition number $\sim O(1 + \ln^2(H/h))$, where H is subdomain size and h is element size, for the optimal (Dirichlet) preconditioner**

- **The coarse problem arises from treatment of the rigid body modes (up to 6 per floating subdomain in elasticity problems and one mode per floating subdomain in potential problems)**

- **A Conjugate Projected Gradient method is used to project out the rigid body modes. The coarse, local Dirichlet, and Neumann problems are solved by direct methods.**

Sandia National Laboratories

BEM Analog of FETI (BETI)

- **A minimization principle is not available, but BEM is inherently a mixed formulation and the flux unknowns can be treated to some extent like the Lagrange multipliers in FETI**

- **The subdomain matrices are unsymmetric and in addition non-orthogonal projection operators are required**

- **An unsymmetric matrix (e.g., bi-conjugate gradient) global solver with 4 projections per iteration is necessary**

- **A write-up of the proposed BETI method will be available shortly**

- **The scalability of this method still needs to be determined**

Sandia National Laboratories

Building a Scalable Code

- **The BETI method will be used as the global solver, to obtain the potential and normal velocities on the subdomain and external boundaries**

- **The existing gridded vortex code will be used as the "subdomain" solver**

  - **Calculate velocity induced on the subdomain boundaries from the subdomain vorticity (prior to global solve)**

  - **Calculate transverse boundary velocities from the normal velocities using the Generalized Helmholtz Decomposition**

  - **Calculate subdomain interior velocities using the GHD**

  - **Advance the vorticity transport equation in time**

Sandia National Laboratories

Present and Near-Term Solver Activities

■ **BETI Solver Development**

- **Assessment of methods to calculate hypersingular BEM coefficients**

- **Development of a BETI solver testbed**

- **Investigation of possible mathematical derivation of BETI scalability**

Present and Near-Term Activities (cont'd)

■ **Gridded Vortex Code Development**

   - **Incorporation of adaptive singular numerical quadrature
methods for 3D coefficient evaluation**

   - **Development of a parallelized version (for use as the subdomain
solver)**

   - **Development of 3D boundary condition options**

Sandia National Laboratories

3D Benchmark Calculation

- ■ **The purpose is to evaluate current capabilities for large interior transport problems and allow future comparisons with the BETI solver at the lower end of its targeted capabilities. This evaluation includes the degree to which turbulence can be captured in a large interior transport problem.**

- ■ **The GILA code (a fast-running FE large-eddy simulation code with statistics package) has been selected for this benchmark**

- ■ **A full-scale, bio-aerosol mixing test (the 911-Bio Advanced Concept Technology Demonstration test sponsored by the DOD CP office) will be analyzed**

- ■ **This work is being done in conjunction with a separate LDRD to improve/develop GILA statistics and plotting packages**

Sandia National Laboratories

Impact of the BETI Method

■ **Success of BETI methods would clearly constitute a major breakthrough for multizone BEM, extending the practical number of zones that can be modeled by a couple orders of magnitude.**

■ **The BETI method will also allow the total number of degrees of freedom that can be treated to increase up to the point that the size of the coarse problem begins to dominate the scalability. At that point the treatment of the coarse problem will have to be revisited.**

Sandia National Laboratories